

Effect of the nonparabolic mass on the electron confinement in arbitrarily shaped quantum wells

Wei-quan Chen and Thorwald G. Andersson

Department of Physics, Chalmers University of Technology, S-412 96 Göteborg, Sweden

(Received 18 April 1991)

A numerical technique for the calculation of electron eigenstates in one-dimensional potential profiles has been improved by including the nonparabolicity of electrons and the material dependence of effective mass in heterostructures. The method is demonstrated for GaAs/Al_xGa_{1-x}As quantum wells, showing its effectiveness and excellent agreement with experiment. It was found that the magnitude of the effective mass and the nonparabolicity have a significant influence on the confinement energy, especially for narrow wells.

Over the past few years, considerable interest has developed in semiconductor quantum-well (QW) and superlattice structures because of their physical properties and the potential for electronic and optoelectronic device applications. The physics of quantum-well devices strongly depends on the position of localized states, as well as transitions between confined states and their response to outer fields. The corresponding wave functions are governed primarily by the shape of the potential, but also the electronic structure of the material in the well and barriers. In real device structure the potential shape as well is usually modified by an applied electric field or optic excitation.

In the epitaxial growth of a heterostructure the physics behind it is reduced to thicknesses and compositions of the material layers. Small deviations from the desired structure due to fluctuation in growth parameters introduce a modification of the wave functions. Therefore accurate calculation of eigenstates for quantum wells with arbitrary potential profiles is needed not only to relate the growth of a layered structure to the position of confined levels, but also to model devices. Furthermore, it is desirable to avoid heavy computer calculations, which are necessary for first-principles calculations. In this paper we employ a numerical method to calculate the wave function and relate confined levels in an arbitrarily shaped quantum-well structure using a material-dependent effective mass including electron nonparabolicity effects.

Several theoretical models, such as variational,^{1,2} transmission matrices,^{3,4} Monte Carlo,⁵ and phase-shift techniques,^{6,7} have been applied to find the confined levels in wells subject to an applied field. The variational method of Bastard is widely used, but its accuracy and region of validity have been questioned.^{8,9} Monte Carlo calculations used by Singh⁵ are also based on the variational principle. Although ground states can be calculated by the variational methods, they are not convenient for excited states. Recently, a numerical technique was developed by Bloss.⁹ He converted the Schrödinger equation into a set of first-order differential equations, which easily can be solved numerically. But a constant effective mass was used in his calculation for the whole structure of QW's, despite the fact that he has mentioned that

position-dependent masses can be incorporated in his numerical procedures. In reality the effective mass should not only depend on the constituent layers, but also include nonparabolicity effects¹⁰ of electrons in the conduction band, especially for narrow quantum wells.

To calculate the confined levels we start from the effective-mass equation within the envelope function framework,¹¹

$$-(\hbar^2/2)[(1/m^*)\psi']' + V(z)\psi = E\psi, \quad (1)$$

with the boundary condition ψ and ψ'/m^* being continuous at the interfaces. Here the effective mass is position and energy dependent, $m^* = m^*(z, E)$, and $V(z)$ is an arbitrary one-dimensional potential. By defining $Y_1 = \psi$ and $Y_2 = \psi'/m^*$, we convert Eq. (1) into two first-order differential equations

$$Y_1' = m^* Y_2, \quad (2)$$

$$Y_2' = 2[V(z) - E]Y_1/\hbar^2. \quad (3)$$

The potential $V(z) = V_0(z) + eFz$ where $V_0(z)$ is an arbitrary potential and F is an applied electric field. To calculate the eigenenergies and eigenfunctions we solved this set of equations by the standard numerical procedures used by Bloss,⁹ here $\psi = 0$ at boundaries which are sufficiently far away from the well so that the position of the boundaries do not influence the confined levels. A calculation was made for a square GaAs/Al_xGa_{1-x}As single quantum well (SQW), using the mass to be described in Eq. (5) and $F = 0$. The result obtained was found to be the same as for the three-band Bastard model.¹² The calculation is shown in Fig. 1, illustrating a SQW structure with confinement energies and the square of the wave functions $|\psi(z)|^2$.

In the evaluation of quantum-well electron confinement energies, nonparabolicity effects have been included in the effective mass for the well material m^* in different ways. The lowest-order correction is

$$m^*/m_\Gamma^* = (1 + \alpha E), \quad (4)$$

where m_Γ^* is the effective mass in the Γ point, α is a constant, and E is the energy above the conduction-band (CB) edge. In Bastard's three-band calculation,¹³ Kane's

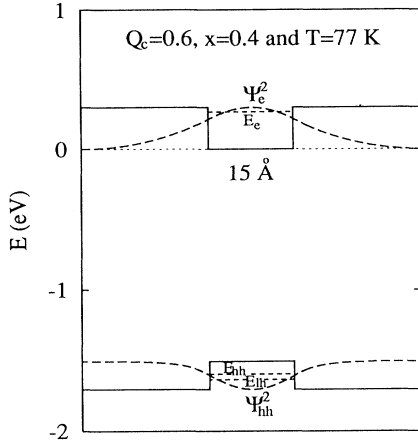


FIG. 1. The conduction and valence band for a GaAs/Al_xGa_{1-x}As single quantum well. Electron and hole confinement energies and the square of the ground-state wave functions are shown. The parameters used in the calculation are shown in the figure.

bulk dispersion relation¹⁴ was used to give the effective mass

$$m^*/m_{\Gamma}^* = (m_0/m_{\Gamma}^*) \left\{ 1 + \frac{2}{3} m_0 P^2 / [2/(E + E_g) + 1/(E + E_g + \Delta_{s.o.})] \right\}^{-1}, \quad (5)$$

where P is Kane's matrix element¹⁴ (describing the coupling between the valence and conduction bands), E_g is the band gap, and $\Delta_{s.o.}$ is the spin-orbit split energy. Later, Ekenberg proposed a more accurate formula for the effective mass,¹⁰

$$m^*/m_{\Gamma}^* = [1 - (1 - 4\alpha E)^{1/2}] / 2\alpha E, \quad (6)$$

in which the parameter α_0 was determined¹⁰ from a 14-band $\mathbf{k} \cdot \mathbf{p}$ calculation, where $\alpha = -(2m_{\Gamma}^*/\hbar^2)^2 \alpha_0 = 0.642 \text{ eV}^{-1}$ for GaAs. We compare these three cases for GaAs in Fig. 2(a). As shown, the difference between them is small at a low confinement energy, so the simple Eq. (4), which is actually the second-order expansion of Eq. (6) by αE ($\alpha E \ll 1$), is good enough for $E < 50 \text{ meV}$. At higher energies the difference increases and is more than 5% at 100 meV above the CB edge. As shown in the same figure, the contribution given by Eq. (6) increases strongly above 100 meV compared to the simple nonparabolic corrections. To illustrate the influence of the position-dependent and nonparabolicity masses on the level of electron confinement energies, we made a series of calculations on GaAs/Al_xGa_{1-x}As quantum wells. In Fig. 2(b) shown is the difference between the electron ground-state energies when using (i) nonparabolic masses [Eqs. (4)–(6)] as well as the position-independent parabolic mass for the well material (nonparabolicity correction for the barrier material was neglected because of its minor contribution to the final results) and (ii) a constant mass in

the whole structure as Bloss.⁹ As shown the error is significant (one example of the error shown by Kim, Gustafson, and Thylen¹⁵ for a single GaAs/Al_{0.3}Ga_{0.7}As QW with a well thickness of 100 Å is consistent with our result), especially for narrow wells. However, the energy differences obtained by different position-dependent masses are small. Equations (4) and (5) as well as the simple parabolic mass can be used with good accuracy for GaAs/Al_xGa_{1-x}As QW's. Evidently, Eq. (6) creates a result that is significant for narrow quantum wells, more than 2-meV correction for wells below 50 Å. For a QW composed of other narrow-band-gap materials where the nonparabolicity effect is more significant, Eq. (6) is expected to create a result having an obvious difference from that given by other mass formulas.

Figure 3 shows wave-function and confined energies for a coupled double-quantum-well structure for the cases with and without an applied field. Here the coupling of the wave functions split the ground state into two levels.

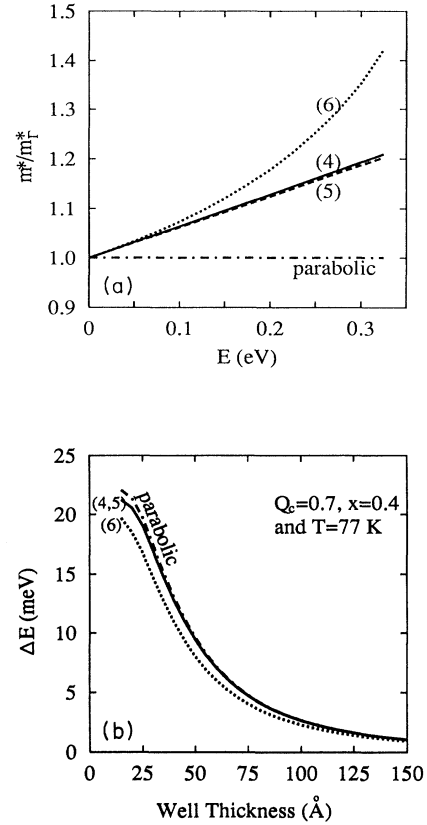


FIG. 2(a). Comparison of variation in the ratio m^*/m_{Γ}^* as a function of confinement energy E in a GaAs/Al_xGa_{1-x}As quantum well. Here m_{Γ}^* is the electron mass at the GaAs conduction-band-minimum. Numbers refer to the equations in the text. (b) The deviation ΔE of the electron ground-state energy, with reference to a position-independent mass, as a function of the GaAs/Al_xGa_{1-x}As SQW thickness. The numbers refer to Eqs. (4)–(6) and the case for the parabolic mass is shown by the dot-dashed line.

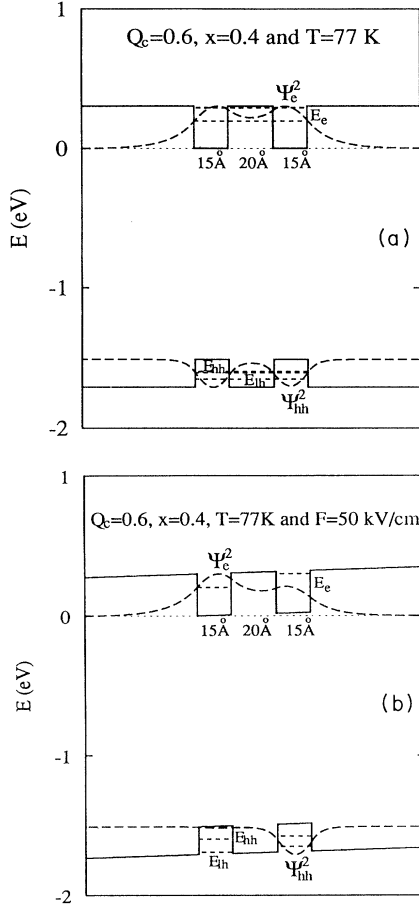


FIG. 3. The same as in Fig. 1 for (a) a coupled GaAs/Al_xGa_{1-x}As double-quantum-well structure and (b) under an applied electric field.

An applied field reduces the coupling and localizes the probability distribution of the wave functions to different sides of the wells. The influence on the SQW luminescence peak (Stark shift) is modeled in Fig. 4, showing good agreement between our calculation (solid curve) and the experimental points¹⁶ (open circles), where the exciton binding energy was not involved because it is small. The inset in Fig. 4 shows the shift of the ground-state

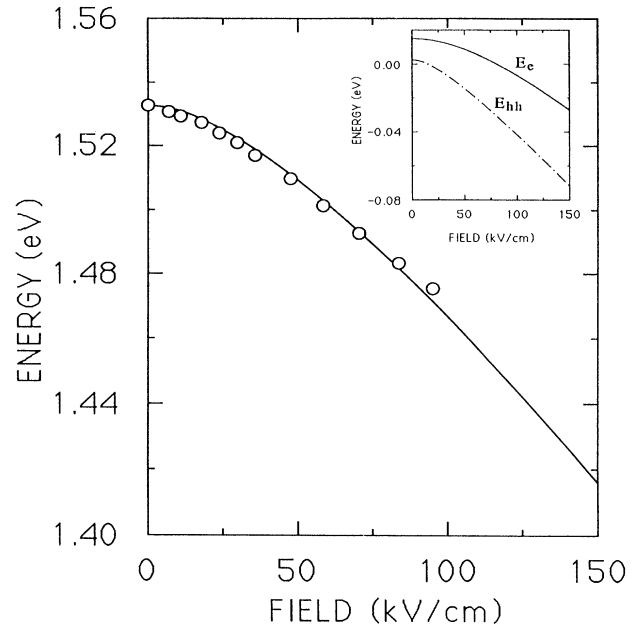


FIG. 4. Theoretical curve (solid line) and experimental points of the luminescence peak shift (Stark shift) for a GaAs/Al_xGa_{1-x}As single quantum well ($L_w = 160 \text{ \AA}$) at a temperature of 5 K, from Ref. 16. Inset: the calculated energy shift of ground-state electron and heavy-hole confinement energies (with reference to the midpoint of the well) as a function of the applied electric field.

electron and heavy-hole confinement energies (E_e and E_{hh} , respectively) as a function of applied electric field. From this we conclude that the method gives a very accurate prediction of both position of confined energies and the relative occupancy $|\Psi(z)|^2$ of an electron (or hole).

By using the wave functions obtained $\psi_e(z)$ and $\psi_h(z)$, the 1S exciton binding energy can also be included in our method by a variational treatment.¹⁷⁻¹⁹ Here the exciton binding energy can be obtained by the minimization of the variational energy $E(\alpha)$ with respect to α :

$$E(\alpha) = \frac{\hbar^2 \alpha^2}{2\mu} - \frac{4\alpha^2 e^2}{\kappa} \int_{-\infty}^{\infty} dz_e \int_{-\infty}^{\infty} dz_h \psi_e^2(z_e) \psi_h^2(z_h) |z_e - z_h| \left[\frac{\pi}{2} [H_1(2\alpha|z_e - z_h|) - N_1(2\alpha|z_e - z_h|)] - 1 \right],$$

where μ is the two-dimensional (in-plane) exciton reduced mass, κ is the static dielectric constant, and H_1 and N_1 are first-order Sturve¹⁹ and Neumann functions, respectively.

In summary, we have improved a numerical technique for the calculation of arbitrarily shaped quantum wells by

including material-dependent effective masses and non-parabolicity effects. The application of this method to a QW subject of an applied electric field has given good agreement between our calculation and the experimental data, even if some factors were neglected, such as exciton binding energy and the mixing effect of bulk Γ and X

states^{20,21} [which has been proved to be negligible for isolated wells in electric fields $(0-5) \times 10^5$ V/cm]. This method is comparatively simple and effective for general use without very extensive computer calculations. Moreover, we find that the use of a constant (position-independent) mass causes a large error, especially for narrow wells. Ekenberg's mass formula,¹⁰ from the 14-band

$\mathbf{k} \cdot \mathbf{p}$ calculation, must be used for narrow, less than 50 Å wide, GaAs/Al_xGa_{1-x}As QW's or excited states.

The Swedish National Board for Technical Development (STU) and the Swedish National Science Research Council (NFR) are acknowledged for financial support.

¹E. J. Austin and M. Jaros, *J. Phys. C* **19**, 533 (1986).

²G. Bastard, E. E. Mendez, L. L. Chang, and L. Esaki, *Phys. Rev. B* **28**, 3241 (1983).

³A. Harwit and J. S. Harris, Jr., *Appl. Phys. Lett.* **50**, 685 (1987).

⁴P. W. A. McIlroy, *J. Appl. Phys.* **59**, 3532 (1986).

⁵J. Singh, *Appl. Phys. Lett.* **48**, 434 (1986).

⁶E. J. Austin and M. Jaros, *Phys. Rev. B* **31**, 5569 (1985).

⁷E. J. Austin and M. Jaros, *Appl. Phys. Lett.* **47**, 274 (1985).

⁸Ajoy K. Ghatak, *IEEE J. Quantum Electron.* **QE-24**, 1524 (1988).

⁹W. L. Bloss, *J. Appl. Phys.* **65**, 4789 (1989).

¹⁰U. Ekenberg, *Phys. Rev. B* **40**, 7714 (1989).

¹¹Peng-fei Yuh and K. L. Wang, *Phys. Rev. B* **38**, 13 307 (1988).

¹²G. Bastard, in *Molecular Beam Epitaxy and Heterostructures*, Vol. 87 of *NATO Advanced Study Institute Series E*, edited by L. L. Chang and K. Ploog (Nijhoff, Dordrecht, 1985), pp.

381-423, and references therein.

¹³G. Bastard and J. A. Brum, *IEEE J. Quantum Electron.* **QE-22**, 1625 (1986).

¹⁴E. O. Kane, *J. Phys. Chem. Solids*, **1**, 249 (1957).

¹⁵I. Kim, T. K. Gustafson, and L. Thylen, *Appl. Phys. Lett.* **57**, 285 (1990).

¹⁶L. Vina, E. E. Mendez, W. I. Wang, L. L. Chang, and L. Esaki, *J. Phys. C* **20**, 2803 (1987).

¹⁷G. Priester, G. Allan, and H. Lannoo, *Phys. Rev. B* **30**, 7302 (1984).

¹⁸J. A. Brum and G. Bastard, *Phys. Rev. B* **31**, 3893 (1985).

¹⁹J. A. Brum, G. Priester, and G. Allan, *Phys. Rev. B* **32**, 2378 (1985).

²⁰J. P. Hagon, M. Jaros, and D. C. Herbert, *Phys. Rev. B* **40**, 6420 (1989).

²¹L. D. L. Brown, M. Jaros, and D. Ninno, *Phys. Rev. B* **36**, 2935 (1987).